Tuning order in disorder

Evan Ma

Recent research has revealed considerable diversity in the short-range ordering of metallic glass, identifying favoured and unfavoured local atomic configurations coexisting in an inhomogeneous amorphous structure. Tailoring the population of these local motifs may selectively enhance a desired property.

The materials science paradigm of 'microstructure determines properties' has been successful in explaining and predicting the behaviour of conventional alloys. This is because these polycrystalline alloys contain a plethora of property-controlling microstructural features, such as grains, second-phase precipitates, interfaces, dislocations, twins and stacking faults, which can all be routinely identified under a microscope and purposely manipulated during alloy processing. In contrast, monolithic metallic glasses (MGs) always appear amorphous with no discernible microstructure, invariably displaying a maze-like pattern when examined under a high-resolution transmission electron microscope[1,2]. Yet, widely different properties have been reported for MGs of different (sometimes even similar) alloy compositions, or for MGs of the same composition but with different processing history[3]. Moreover, recent property mapping on the surface of an MG has also revealed mechanical (elastic and plastic) heterogeneity on the nanometre scale[4,5]. One probable contributor to this variability is the different types, and degrees, of structural order developed and distributed in the glass[6,7]. A major challenge is therefore to decipher the structural differences in these seemingly structureless alloys, and establish a causal link between the key local structures and macroscopic properties. As explored in this Commentary, the recently uncovered variety of local atomic environments sheds new light, from the atomic packing perspective, on the long-existing but vague picture of 'solid-like' and 'liquid-like' regions in MGs. These structural inhomogeneities may be tuned in a controllable manner, to improve the properties of an MG, such as its deformability or stability.

Spectrum of atomic-packing motifs

Metallic glasses, while macroscopically uniform, are not truly homogeneous as their disordered nature may suggest. The internal structure of MGs was initially described as dense random packing of hard spheres[8]. Research over the years has concluded that while the atomic packing is indeed dense, it cannot be random. Instead, in spite of the lack of long-range order the atoms inside are in a range of distinctly different local atomic configurations at the level of nearest-neighbour coordination, called short-range order (SRO) (see references cited in ref. 7). Such a local structural distribution across a range of SROs, ordered to varying degrees, is schematically depicted in Fig. 1a for an MG, in comparison to its crystalline counterpart. The preponderance of SROs arises because the efficient filling of space with atoms of different sizes necessarily entails topological local order[9]. Meanwhile, metallic atoms are not hard spheres but interact via many-body, 'soft' potentials, and therefore must also prefer chemical local order to select favourable neighbours to lower energy[10]. Moreover, the non-directional nature of metallic bonding, via delocalized electrons, is not compatible with stereochemical units with fixed coordination number and bond angles, such as those in covalently bonded oxide glasses[11]. This leads to an even greater flexibility for the favourable coordination polyhedron: the motif does not necessarily copy the basic building unit in a crystalline intermetallic compound, and can accommodate different numbers of atoms in the nearest-neighbour shell, for example, via geometric distortions to various degrees. In fact, multiple types of motif may also be needed to avoid packing frustration when filling the three-dimensional space[12]. The local order spectrum in Fig. 1a is in stark contrast to a crystalline metal, where nearly all the atoms take the same designated lattice sites, except for a very small fraction of almost identical outliers that are well-defined 'defects' (such as vacancies and dislocations)[13].

The characteristic SRO (the peak) and the entire spectrum also change with MG composition. A recent progress in the foundational understanding of the SRO types is the direct demonstration, based on state-of-the-art experiments and simulations[7,10], that the MG structure can be viewed as composed of interpenetrating quasi-equivalent clusters (coordination polyhedra) that trend towards specific

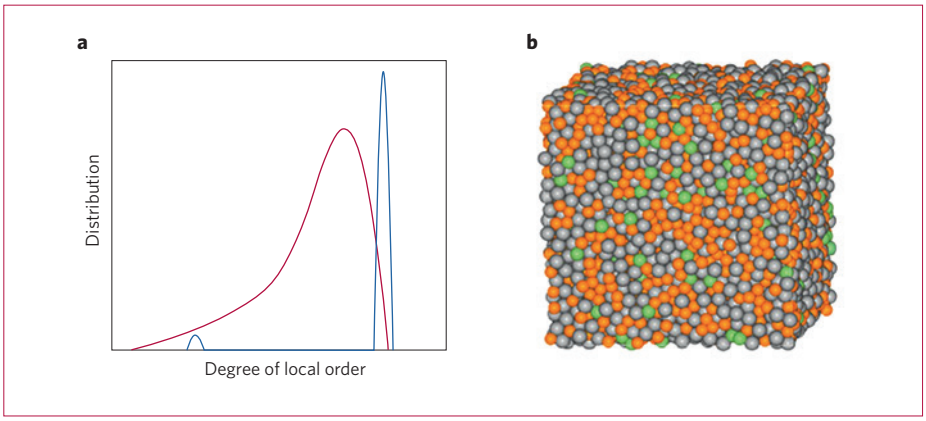

Figure 1 | Local structural variation in an MG versus a crystalline metal. **a**, Schematic illustration contrasting the distribution of local order in MGs (red curve) with conventional crystalline metals (blue curve). The MG structure features varying degrees of short-to-medium-range order. The crystal however has bifurcated local environments composed of a near-perfect lattice (well-defined spike), plus discrete defects such as dislocations and vacancies (small peak). **b**, Dense atomic packing of a 10,000-atom $Cu_{46}Zr_{47}Al_7$ MG configuration, obtained by quenching at 1×10^{10} K s^{-1} from liquid to room temperature in a molecular dynamics simulation (Cu, orange; Zr, grey; Al, green). Panel **a** adapted with permission from ref. 13, © Y. Q. Cheng, J. Ding and E. Ma.

Table 1 | Polytetrahedral Z cluster at each coordination number (CN).

CN	Z cluster	Increasing content of defects in polytetrahedral packing			
8	<0,4,4,0>	<0,5,2,1>	<0,6,0,2>		
9	<0,3,6,0>	<0,4,4,1>	<0,5,2,2>	<0,6,0,3>	
10	<0,2,8,0>	<0,3,6,1>	<0,4,4,2>	<0,5,2,3>	<0,6,0,4>
11	<0,2,8,1>	<0,3,6,2>	<0,4,4,3>	<0,5,2,4>	<0,6,0,5>
12	<0,0,12,0>	<0,2,8,2>	<0,3,6,3>	<0,4,4,4>	<0,5,2,5>
13	<0,1,10,2>	<0,2,8,3>	<0,3,6,4>	<0,4,4,5>	<0,5,2,6>
14	<0,0,12,2>	<0,1,10,3>	<0,2,8,4>	<0,3,6,5>	<0,4,4,6>
15	<0,0,12,3>	<0,1,10,4>	<0,2,8,5>	<0,3,6,6>	<0,4,4,7>
16	<0,0,12,4>	<0,1,10,5>	<0,2,8,6>	<0,3,6,7>	<0,4,4,8>
17	<0,0,12,5>	<0,1,10,6>	<0,2,8,7>	<0,3,6,8>	<0,4,4,9>

Several variations of coordination polyhedra, deviating from the Z cluster towards increasingly diminishing five-fold bonds (from left to right), are also included for each polytetrahedral Z cluster type. Data from ref. 10.

chemically and topologically favourable local configurations[7,10,14–16]. In an MG, for each component (for example, Cu in Cu–Zr MGs) there is a particularly favoured stable atomic size ratio (or effective ratio for the fractions of species needed to make up the nearest-neighbour shell at the alloy composition)[14–16], giving rise to a preferred coordination number (CN). This CN is different from one MG composition to another, and the packing topology of the coordination polyhedra changes accordingly. The locally favoured polyhedra are the polytetrahedral Z clusters[17,18], which are listed in the first column in Table 1 for each CN in the typical range of 8 to 17 (ref. 10). As an example, in the $Cu_{64}Zr_{36}$ MG, the locally favoured motif and therefore the most populous SRO centred on Cu is the Z12 full icosahedra (CN = 12, Voronoi index <0,0,12,0>) (Fig. 2)[19,20]. Moderate deviations (see examples in Table 1) can change the CN = 12 clusters to <0,2,8,2> and <0,3,6,3>, and shift the CN to 11 or 13 (see the middle four types in Fig. 2). In the meantime, Zr tends towards Z16 local packing (CN = 16, Voronoi index <0,0,12,4> in Table 1)[20], such that both species in the alloy simultaneously approach efficient packing in favour of tetrahedral topology[7,10,19,20]. In terms of atomic packing options, the preferable Z clusters in Table 1 may be perceived as fundamental motifs comprising the structural genome of MGs.

With regard to packing motifs, a misconception is to picture them as separated individual clusters, with void-like empty space in between, analogous to some open-structured oxide glasses where networked basic units enclose 'holes'[21]. To clarify, the MGs are categorically different, because they are densely packed 'atomic glasses' (see the configuration example in Fig. 1b), with each atom centring a highly coordinated polyhedron, without regularly spaced cavities. Also, the packing polyhedra are not ideal or perfect in shape[10,20] and are in fact always distorted[12,20] to be accommodated in the overall structure. Another perhaps over-emphasized description in the literature is 'icosahedral ordering', leaving an impression that MGs universally rely on this particular SRO geometry. But as seen in Table 1, CN = 12 full icosahedra are in fact uncommon as the predominant coordination polyhedra[10,20]. Instead it is the five-fold bonds that are truly populous across the board: for all the Z clusters, the third Voronoi index for the number of five-fold faces, is the highest digit. For example, the Z9 cluster (the <0,3,6,0> tri-capped trigonal prism) is not an icosahedron but the five-fold bonds form (distorted) pentagonal bipyramids (a fragment of icosahedron). In other words, the underlying principle is efficient polytetrahedral packing[17,18] preferring triangulated faces and minimizing the content of extrinsic defects that diminish rotational symmetry; five-fold bonds, rather than necessarily completed icosahedra, are what is implicated via the descriptor 'icosahedral order'[10,20].

While any given MG would tend to maximize its favourable SROs, these locally favoured structures are accompanied by a range of motifs at the other end of the curve in Fig. 1, as also demonstrated in Fig. 2 and Table 1. Most of these latter polyhedra are geometrically unfavoured motifs (GUMs) in the local structural spectrum, but nevertheless needed for spacing filling and connecting the backbone structures. Many may simply be less ordered regions retained during fast liquid cooling. These GUMs are those in Table 1 that either deviate significantly (that is, towards the far right in the corresponding row) from the Z cluster preferred at a given CN, or are under- (or over-) coordinated to unusually low (or high) CNs. Although each type of these clusters may be of low population, together they may constitute a fairly large fraction (in the group marked as 'others' in Fig. 2). In particular, those most disordered (unfavoured) local environments near the tail end (see the red curve in Fig. 1a) may be relatively unstable and hence more conducive to reconfiguring via thermal- or stress-induced relaxation. Such structural heterogeneities have impact on properties, as explored further in the next section.

Implications on properties

The analysis above suggests that one approach to dissect the structural basis of MG properties is to start from the two opposite ends of the spectrum in Fig. 1a. The first group is of course based on the majority SRO around the peak in the red distribution curve; these characteristic SROs have indeed been the focal point of many previous studies (for example, see references cited in ref. 10). As the locally favoured structures interconnect to constitute the building blocks of the MG backbone, their development is believed to be responsible for the stability of the MG. For example, much has been said about the role of the favoured local order in affecting the potential energy[22] (and its derivative, the temperature-dependent specific heat[23,24]), as well as in influencing the barrier to crystallization[25,26]. The preferred SRO also elevates the stiffness and correlates with local elastic modulus and its nanoscale heterogeneity[20], and slows down the relaxation dynamics[27]. Recently, the increasing order developed on cooling of a supercooled MG-forming liquid was directly linked to the continuously increasing energy barrier for relaxation events[23,24], in light of the Adam–Gibbs theory, to rationalize the non-Arrhenius behaviour of the viscosity. A new experiment in fact suggested that the rate of this structural ordering as a function of temperature is a signature of the kinetic fragility of the liquid[28]. Molecular dynamics simulations lend support to this conjecture, by showing that two deeply supercooled liquids with obviously different temperature dependence of the viscosity exhibit contrasting trends in the evolving short-to-medium-range order[23,24]. It seems that even though viscosity may involve complex correlations over dynamic length scales that are different from structural ones[29], ordering appears to be a useful indicator and suggestive of possible structural mechanisms.

We now direct our attention to the group of motifs furthest away from the

locally favoured ones, the GUMs' side of the structural spectrum. As mentioned previously, GUMs are inevitable in any given MG (Fig. 2), and can also be generated at the expense of other SROs (for example, under deformation). Intuitively, GUMs are the less stable minority local environments[30], such that they would be more prone to elastic deformation and inelastic relaxation. When a local region contains a high content of GUMs, it can be among the most responsive to stresses[30,31] (either applied or arising due to anisotropy in the structure), thus playing a role analogous to the defects that are well known to mediate diffusion and plastic deformation in a crystal. Of course, there are also major differences from crystalline metals. The MG structure is not bifurcated into lattice and clear-cut defects (blue curve in Fig. 1a). There is also no clear and easy boundary to demarcate which GUMs (and GUM-rich regions) would be actually activated in a particular experiment to carry relaxation and deformation. Moreover, in responding to external stimuli, the atoms in an MG would react cooperatively via collective rearrangements, in lieu of the long-range migration of discrete defects in crystals.

Over the years, MGs have been vaguely pictured to contain liquid-like regions. But the latter have not been clearly and physically defined, as to how liquid-like they are rheologically[32], and their population, location, length scale and geometric arrangements[33]. Our structural perspective here is based on atomic packing: GUMs are compromised configurations, and should be more flexible to enable reconfiguration to reduce energy under external stimuli. Local regions with a high content of GUMs would therefore behave more liquid-like. For affording more flexibility and deformability, it is good news that in any given MG the order developed is non-uniform and locally anisotropic[33], such that an appreciable fraction of atoms are in GUMs and may thus instigate liquid-like regions in multiple locations. This perspective also complements another widely used indicator of structural state, the 'free volume'[34]. On average, GUMs would contain more excess volume; but the new ingredient here is that the disorder in packing adds a tangible structural marker that can be readily monitored and located; the free volume in MGs, on the other hand, is subtle in definition[35] and low in content (of the order of only a fraction of one volume per cent), making it difficult to work with. We also note that GUMs are not always associated with loose packing, and can also be overcrowded atomic arrangements (excess atomic pressure[35]).

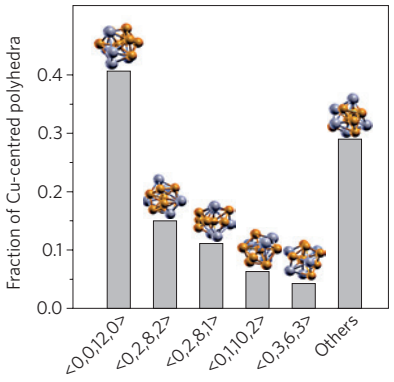

Figure 2 | Coordination polyhedra distribution in a metallic glass. Fractions of various Voronoi polyhedra around Cu atoms in a 32,000-atom molecular dynamics simulation of a $Cu_{64}Zr_{36}$ MG model prepared by quenching at 1×10^9 K s^{-1} from liquid to 300 K. Figure published with permission from Jun Ding, based on data in ref. 20.

As a specific example demonstrating the role of GUMs in deformability, Fig. 3 shows that in the simulation box of a $Cu_{64}Zr_{36}$ MG model, the (Cu and Zr) atoms with the strongest participation in the soft vibrational modes (the 1% modes with the lowest frequency and hence weakest spring constants) are mostly inside GUMs[30]. They are heterogeneously distributed in the system to form nanometre-scale 'soft spots'[30]. In Fig. 4, on shearing the model to 10% global strain, the top 10% atoms (both Cu and Zr, white open circles) that have experienced the largest total non-affine atomic strains are displayed. We observe that these top-most displaced atoms often coincide with those (bright coloured) soft spots. Taken together, Figs 3 and 4 suggest that the mechanical (elastic and plastic) heterogeneity exhibits some degree of correlation with the structural inhomogeneities: at least the highest deformation propensity appears to arise from GUM environments where atoms with the lowest packing order reside. Conversely, the stiff backbone of an MG is a network rich in interpenetrating favourable motifs, corresponding to high-modulus regions[20]. This provides a structural basis for explaining the large and puzzling spatial mechanical property variations mapped out in experiments, such as the nanometre-scale inhomogeneity in the contact resonance frequency and the non-uniform distribution of local energy dissipation[4,5].

Although such a structure–behaviour correlation is interesting, it is rudimentary and on a statistical basis only (see later discussions on outstanding questions in section 'Challenges ahead'). Nevertheless, in general a trend should hold that when it comes to deformability, the more GUMs, the better. This has been exploited in processing MGs for better plasticity. For example, faster quenching of the liquid in MG preparation, which retains more GUMs, and hence more soft spots and more fertile sites for shear transformation in the as-cast MG structure (previously depicted as retaining more free volume and liquid-like regions), is known to increase the fracture toughness[36]. One can also purposely introduce numerous highly disordered regions as interfaces between nanometre-sized MG 'grains'; in such a 'nanoglass' the interfaces help spread plastic flow to the entire sample volume[37]. Another strategy to tune the MG structural distribution is by selecting suitable alloy compositions. One example was the Zr-rich compositions in the Cu–Zr system[36]. In that case the CN around Cu shifts towards 10 (refs 10,27), where full icosahedra diminish. The resulting motif spectrum offers a wider variety of SROs that are amenable to being turned into GUMs under stresses. This activates shear transformations and strains that are more spread out[36], to dissipate energy. A resulting Zr-based bulk MG was found to show record-high damage tolerance[36]. When severe strain localization via shear banding is suppressed in small samples at certain MG compositions[38], spatially distributed shear transformations can be sufficient to carry the imposed strain rate: an MG could even exhibit ductile rupture, that is, the necked region was eventually drawn to a point before fracture, in uniaxial tension at room temperature[39].

Rejuvenation versus crystallization

Continuing the thought above, another obvious strategy to improve deformability is to use externally driven processes to introduce more disorder into a relaxed MG. This 'rejuvenates' the glass structure, skewing the SROs towards more GUMs and furthering their degree of disorder. Indeed, several previous studies improved the plasticity of MGs via pathways that proliferate GUMs. For example, MGs subjected to ion irradiation are expected to become more disordered; such an MG behaves like a ductile metal and the necking in tension becomes pronounced at room temperature[40]. Mechanical loading (pre-straining) also led to rejuvenation[38,41], thanks to many stress-driven shear transformation events. An increasing number of relaxed local configurations are turned into GUMs, and existing GUMs are driven towards higher degree of disorder. Both irradiation and deformation (and fast quenching as well) lead the glass to a state of higher

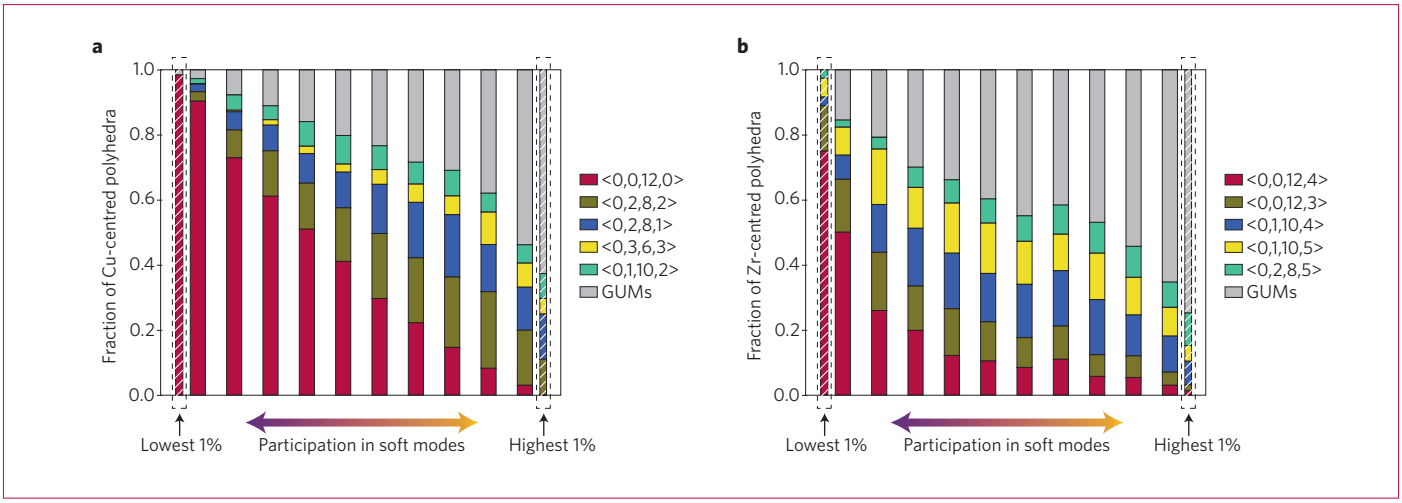

Figure 3 | Atomic contributions to soft vibrational modes in simulated $Cu_{64}Zr_{36}$ MG. Atoms in different local packing environments contribute differently. **a**,**b**, For Cu atoms in **a** (and for Zr atoms in **b**), each of the ten solid bars represent a bin that contains 10% of all the Cu (or Zr) atoms in the system, and displays the make-up of these atoms (different colours for atoms at the centre of the different types of coordination polyhedra). From left to right, the bins are ordered from the lowest to the highest participation probability in soft modes. Two additional bars in dashed boxes are for the 1% of atoms with the lowest participation, and the highest participation. Atoms that participate the most in soft modes (bars towards the right) are increasingly dominated by Cu (or Zr) atoms in GUMs. Figure adapted with permission from ref. 30, NAS.

energy and improved deformability, but lower stability.

An underappreciated outcome of shear transformations, along with producing strains and stress-driven rejuvenation, is ordering and even crystallization[38], an energy-lowering alternative driven by stresses. Here, we draw attention to the notion that, in addition to inducing a homogeneous (affine) shape change, shear transformation has an aspect of diffusion-like atomic rearrangements. This is mathematically seen from the decomposition of relative atomic displacements into affine and non-affine components[42,43]. For a collection of atoms, the repeated non-affine displacements accrue approximately linearly with time[43], a parallel of the defining characteristic of mean squared displacement in thermal diffusion. This accumulative effect is more likely when the deformation is gentle and in multiple stress–strain cycles[43], in lieu of a large-magnitude shear straight to failure (fracture). In other words, given enough opportunities the stresses can shake the atoms and nudge them collectively across barriers to reach different basins on the potential energy landscape.

More specifically, shear-dominant tensorial stress can lower energy barriers significantly[44], as the activated volume in shear transformations is relatively large, involving many tens or even hundreds of atoms[38]. This enables new 'menu options' to become accessible, including higher-energy states (rejuvenation) as well as lower-energy basins. For the latter route, the more-ordered patches of atoms can link up to fall in a new metastable state, gradually traversing the phase-space distance towards the stable state, even though they do not migrate in the absence of temperature-induced atomic mobility. The densely packed MGs usually do not exhibit polyamorphism (akin to the first-order transition between different crystal polymorphs that exhibit different symmetry and molar volume at the same composition), except in a handful of cases where a higher-density form can be reached under high pressure due to the delocalization of the 4*f* electrons, the first example being a cerium-containing MG[45]. But the ordered atoms can be collectively realigned by the stresses to form a nanocrystal[43]. This is thus a new mode of highly cooperative crystallization that can happen at any temperature, without heating-induced thermal diffusion of individual atoms. Recently, it has been found that the nanocrystals can indeed be created under deformation conditions that do not incur a temperature rise[38,46], and they influence shear bands, block crack propagation and improve damage tolerance[43]. Note that stress-driven crystallization evades the trade-off incurred via the rejuvenation route, which produces a more unstable glass that is subject to structural relaxation and hence property changes over time. It is therefore yet another interesting twist in taking advantage of order within disorder.

Challenges ahead

Several links in the knowledge chain of structure–property relations remain missing. The first outstanding issue is that, while the preferred SRO has been confirmed, the ultimate degree and extent of its development in a real-world MG remains undetermined. So far, the most ordered configurations came from computer simulations[7,10], which are severely limited in simulation time and length scales such that the cooling rate is orders of magnitude faster than experiments[20,47]. This precludes a glass configuration truly representative of a laboratory MG. One would naturally question if there is a saturation of the dominant SRO type[20], and at what level other types persist, including the GUMs that connect into liquid-like regions.

Second, the extended order, and the organization of SRO motifs, on the length scale of a couple of nanometres (medium-range order, MRO) and beyond, is only beginning to be explored[10,32]. The poor understanding of MRO at present is particularly unfortunate for several reasons. The MRO could be the tell-tale difference between a glass and its crystal counterpart: in some systems the relatively strong chemical affinity renders the SRO in the glass almost identical to that in the crystal[10]. Also, MRO covers a length scale comparable to the size of a shear transformation zone, the elemental block for relaxation and deformation[30]. Moreover, MRO would be important in understanding the structural origin of property heterogeneity observed in MGs. Finally, MRO is a key link in the percolation to construct the backbone. How to identify recognizable MRO patterns in a more unambiguous way, how to define and

characterize the critical percolation and the resultant backbone beyond the nanometre scale, and how the behaviour of this backbone is related to the transition points (for example, glass transition and yielding), are all challenging questions that need to be addressed.

The third question concerns whether Figs 3 and 4 are truly indicative of a robust structure–property relationship. When a shear transformation is initiated, the first several trigger atoms[48] are displaced so much that they may appear to only weakly correlate with the original soft spots in the structure. Also, with increasing stress and strain, more and more GUMs are activated, together with many locally favoured motifs that are being disordered. In other words, starting from the atoms that are the easiest to cooperate, deformation works its way towards the more unwilling side of the structural spectrum. Eventually, all the atoms will be activated to 'flow', regardless of their original local structure: an extreme case is inside the shear band of a plastically deforming MG. As such, the correlation observed in Figs 3 and 4 is a snapshot captured along the way, in a deformation stage when the soft spots and associated GUMs exhibit a higher propensity to record displacements. In Fig. 4, there are soft spots that have not experienced large displacements, and also favourable SRO motifs (full icosahedra in this particular MG) that have. So a one-to-one correspondence is not found nor expected. There must be factors beyond local SROs that come into play, in controlling the propensity of shear transformation. This includes what the neighbouring motifs are and how they interconnect with one another, which underscores again the need for an account of the contribution of MROs. One also needs to know how the local region relates to already deformed ones, and how it couples with the applied tensorial stress. In any case, the correlation here with packing order employing the simple and degenerate Voronoi index can only serve as a starting point.

This brings up the fourth issue, namely the possibility of a better structural indicator that may enable a quantitative correlation with properties. In this context, we note that a measure of disorder often used in the field of glass science is the fictive, or effective, temperature[49]. This metric is useful for modelling, but not for directly revealing the structure per se. Since the population of local clusters is a function of temperature, one can now use GUMs as a concrete and detailed way of expressing the physical make-up of fictive temperature. However, such a topological indicator would be difficult to quantify in mathematical equations. A case can be made for the need for a more powerful composite structural indicator. Ideally, this new metric would not only describe the features and extent of configurational disorder (including topology and free volume), but also reflect other more functionally oriented parameters that have implicit connections with structure, such as the atomic-level stresses, potential energy (and fictive temperature), local elastic modulus, vibrational amplitudes, and activation barriers along the various relaxation pathways in the energy landscape[48]. Such a structural variable needs to be amenable to quantitative predictions, which currently remains a major challenge as reflected by the lack of a crystal-plasticity-like theory to link MG structure to mechanical properties.

The fifth challenge stems from the limitations suffered by current processing routes in rejuvenating the MG structure throughout the whole sample. Rapid liquid quenching, or irradiation of an MG with high-energy beams, limits the sample size that can be treated to the micrometre scale, whereas deformation causes shape change and often localizes strains in deformation bands where flaws may be generated. One desires a non-destructive, isotropic and inexpensive method that can be applied to bulk samples. For example, it is conceivable that carefully designed cycles of (pulsed current) heating (for example, into the supercooled liquid region) followed by rapid self-quenching[50] may possibly rejuvenate some MG structures for improved deformability.

Finally, we note that there is a limit as to how far one can reach in tailoring the deformability of MGs by tuning the internal order alone. For example, there will be MGs that remain brittle no matter how fast the liquid is cooled in preparing the sample, or whichever way the composition is adjusted

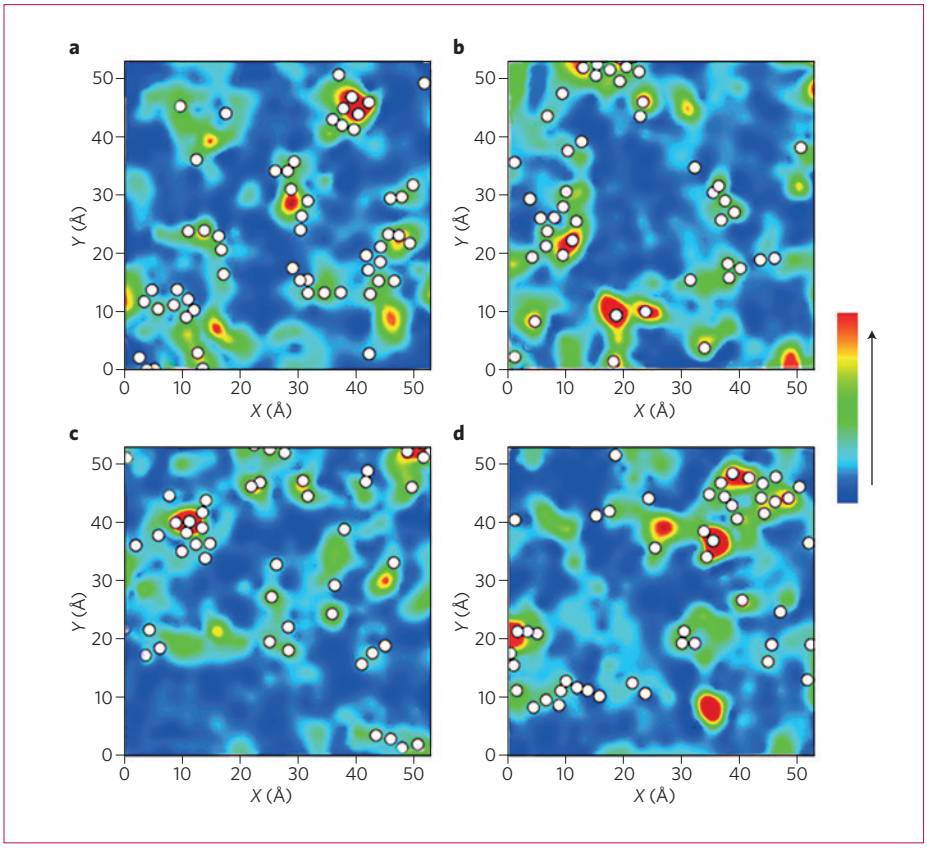

Figure 4 | Contour maps showing the heterogeneous spatial distribution of Cu and Zr atoms that participate the most in soft modes, correlated with those that contribute the most to deformation strain. The $Cu_{64}Zr_{36}$ MG model was prepared via cooling at 1×10^{9} K s^{-1} in a molecular dynamics simulation. **a**–**d**, The four sampled representative thin slabs each has a thickness of 2.5 Å. The colours indicate the different degrees of participation (increasing along the arrow in the colour scale bar) in soft vibrational modes. The white circles mark the locations of the top 10% of the local motifs that have experienced the most accumulative non-affine strains, on athermal quasistatic shear of the simulation box to a global strain of 5%. Constructed from data reported in ref. 30.

in that alloy system. To illustrate this point, we use a macroscopic parameter, Poisson's ratio (ν, which inversely scales with the G/B ratio, where G is the shear modulus and B bulk modulus), as an indicator of MG deformability and toughness (liquid 'flows' and has a ν of 0.5, whereas brittle ceramics have low ν approaching 0.2)[51]. The modulus can be decomposed into two contributing terms: one intrinsic from the constituent elements (subscript e; the Born term[52] that can be calculated from affine deformation, such as for the crystalline counterpart of the MG), and the other dependent on the particular glassy configuration prepared (subscript c; a negative term arising from non-affine deformation[33,42,43,53]). The G/B ratio is then controlled by the product of the following two terms

$$\frac{G}{B} = \frac{G_e + G_c}{B_e + B_c} \approx \frac{G_e}{B_e}\left(1 + \frac{G_c}{G_e}\right)$$

as B is not sensitive to the details of the structure such that B_c/B_e can be neglected[51,52]. If the MG is made of brittle elements, the chemical make-up term G_e/B_e would be too large that it overshadows the atomic-configuration term G_c/G_e (ref. 51). As a result, for elevating the plasticity one needs to consider element selection in addition to structural optimization.

For MGs made from primary components that have similar G_e/B_e, such as Cu and Zr, a lower G_c/G_e (more GUMs) can make a major difference, as revealed in computer simulations[51]. However, the root cause remains unsettled. One could argue from the angle of motif distribution, as discussed above. But each alloy has its own preferred motifs, and as indicated earlier always contains a high fraction of five-fold bonds. So it remains challenging to sort out exactly why different compositions entail different magnitude of G_c/G_e and propensity for shear transformation (and associated GUM production). In this regard, one would desire a universal metric that quantitatively reports on the overall configurational contributions to G_c/G_e, to facilitate the comparison of different MGs and understand why sometimes the plasticity can be sensitively dependent on alloy composition (for example, the wide variation of fracture toughness among MGs)[3,36].

In summary, the variety of local order identified in MGs is projected to preferentially influence different glass properties. The populous SROs that characterize the locally favoured configurations are primarily responsible for the thermodynamic and kinetic stability of the amorphous alloy, whereas the coexisting GUMs impart more flexibility to facilitate relaxation events. In particular, a packing-configuration-oriented indicator, that is, the heterogeneities with enriched GUMs, provides a tractable structural descriptor of the liquid-like regions (or locations where the average free-volume content is higher). Statistically speaking, these locally unfavoured regions tend to be softer and add propensity for relaxation. Structural design or rejuvenation routes that elevate their population or boost their responses can therefore improve deformability. Opportunities abound in utilizing the ability to judiciously control the local order inhomogeneities to derive better properties. In our pursuit of concrete structure–property relations thus far, one-to-one causal correlations have been difficult to come by, because the structural indicator used tends to accentuate one particular aspect of the MG structure and is usually not suitable for quantitative derivation of properties. This underscores the pressing need for distilling tell-tale structural metrics that have a predictive power on par with those for crystalline metals (such as dislocation density and Burgers vector). ❐

Evan Ma is in the Department of Materials Science and Engineering, Johns Hopkins University, Baltimore, Maryland 21218, USA.
e-mail: ema@jhu.edu

References

1. Hirata, A. *et al. Nature Mater.* **10,** 28–33 (2011).
2. Ma, E. & Zhang, Z. *Nature Mater.* **10,** 10–11 (2011).
3. Greer, A. L. *in Physical Metallurgy* (eds Laughlin, D. E. & Hono, K.) 5th edn 305–385 (Elsevier, 2014).
4. Wagner, H. *et al. Nature Mater.* **10,** 439–442 (2011).
5. Liu, Y. H. *et al. Phys. Rev. Lett.* **106,** 125504 (2011).
6. Finney, J. L. *Proc. R. Soc. Lond. A* **319,** 479 (1970).
7. Sheng, H. W., Luo, W. K., Alamgir, F. M., Bai, J. M. & Ma, E. *Nature* **439,** 419–425 (2006).
8. Bernal, J. D. *Nature* **185,** 68–70 (1960).
9. Torquato, S., Truskett, T. M. & Debenedetti, P. G. *Phys. Rev. Lett.* **84,** 2064–2067 (2000).
10. Cheng, Y. Q. & Ma, E. *Prog. Mater. Sci.* **56,** 379–473 (2011).
11. Zheng, K. *et al. Nature Commun.* **1,** 24 (2010).
12. Hirata, A. *et al. Science* **26,** 376–379 (2013).
13. Cheng, Y. Q., Ding, J. & Ma, E. *Mater. Res. Lett.* **1,** 3–12 (2013).
14. Miracle, D. B. & Sanders, W. S. *Philos. Mag.* **83,** 2409–2428 (2003).
15. Miracle, D. B. *Nature Mater.* **3,** 697–702 (2004).
16. Miracle, D. B. *Acta Mater.* **54,** 4317–4336 (2006).
17. Nelson, D. R. & Spaepen, F. in *Solid State Physics-Advances in Research and Applications* (eds Ehrenreich, H. & Turnbull, D.) Vol. 42, 1–90 (Academic, 1989).
18. Nelson, D. R. *Phys. Rev. B* **28,** 5515–5535 (1983).
19. Kramb, R. C., Ward, L. T., Jensen, K. E., Vaia, R. A. & Miracle, D. B. *Acta Mater.* **61,** 2025–2032 (2014).
20. Ding, J., Cheng, Y. & Ma, E. *Acta Mater.* **69,** 343–354 (2014).
21. Guthrie, M. *et al. Phys. Rev. Lett.* **93,** 115502 (2004).
22. Wu, S. Q., Wang, C. Z., Hao, S. G., Zhu, Z. Z. & Ho, K. M. *Appl. Phys. Lett.* **97,** 021901 (2010).
23. Ding, J., Cheng, Y. Q., Sheng, H. & Ma, E. *Phys. Rev. B* **85,** 060201 (2012).
24. Ding, J., Cheng, Y. Q. & Ma, E. *Acta Mater.* **61,** 3130–3140 (2013).
25. Kelton, K. F. *et al. Phys. Rev. Lett.* **90,** 195504 (2003).
26. Shen, Y. T. *et al. Phys. Rev. Lett.* **102,** 057801 (2009).
27. Cheng, Y. Q., Sheng, H. W. & Ma, E. *Phys. Rev. B* **78,** 014207 (2008).
28. Mauro, N. A., Blodgett, M., Johnson, M. L., Vogt, A. J. & Kelton, K. F. *Nature Commun.* **5,** 4616 (2014).
29. Royall, C. P. & Williams, S. R. *Phys. Rep.* **560,** 1–75 (2015).
30. Ding, J., Patinet, S., Falk, M. L., Cheng, Y. & Ma, E. *Proc. Natl Acad. Sci. USA* **111,** 14052–14056 (2014).
31. Cheng, Y. Q., Cao, A. J., Sheng, H. W. & Ma, E. *Acta Mater.* **56,** 5263–5275 (2008).
32. Zhang, Y. *et al. Phys. Rev. B* **90,** 174101 (2014).
33. Dmowski, W., Iwashita, T., Chuang, C. P., Almer, J. & Egami, T. *Phys. Rev. Lett.* **105,** 205502 (2010).
34. Spaepen, F. *Acta Metallurgica* **25,** 407–415 (1977).
35. Egami, T. *JOM* **62,** 70–75 (2010).
36. Xu, J. & Ma, E. *J. Mater. Res.* **29,** 1489–1499 (2014).
37. Gleiter, H. *Beilstein J. Nanotechnol.* **4,** 517–533 (2013).
38. Greer, A. L., Cheng, Y. Q. & Ma, E. *Mater. Sci. Eng. Rep.* **74,** 71–132 (2013).
39. Yi, J., Wang, W. H. & Lewandowski, J. J. *Acta Mater.* **87,** 1–7 (2015).
40. Magagnosc, D. J. *et al. Sci. Rep.* **3,** 1096 (2013).
41. Lee, S. C., Lee, C. M., Yang, J. W. & Lee, J. C. *Scripta Mater.* **58,** 591–594 (2008).
42. Falk, M. L. & Langer, J. S. *Phys. Rev. E* **57,** 7192–7205 (1998).
43. Wang, C. *et al. Proc. Natl Acad. Sci. USA* **110,** 19725–19730 (2013).
44. Lacks, D. J. & Osborne, M. J. *Phys. Rev. Lett.* **93,** 255501 (2004).
45. Sheng, H. W. *et al. Nature Mater.* **6,** 192–197 (2007).
46. Kim, J. J. *et al. Science* **295,** 654–657 (2002).
47. Zhang, F. *et al. Appl. Phys. Lett.* **104,** 061905 (2014).
48. Fan, Y., Iwashita, T. & Egami, T. *Nature Commun.* **5,** 5083 (2014).
49. Haxton, T. K. & Liu, A. J. *Phys. Rev. Lett.* **99,** 195701 (2007).
50. Zaluska, A. & Matyja, H. *Mater. Sci. Eng.* **89,** L11–L13 (1987).
51. Cheng, Y. Q., Cao, A. J. & Ma, E. *Acta Mater.* **57,** 3253–3267 (2009).
52. Cheng, Y. Q. & Ma, E. *Phys. Rev. B* **80,** 064104 (2009).
53. Weaire, D., Ashby, M. F., Logan, J. & Weins, M. J. *Acta Metallurgica* **19,** 779–788 (1971).

Acknowledgements

The author acknowledges contributions from J. Ding, Y. Q. Cheng, H. W. Sheng and M. L. Falk, and support from the US Department of Energy, Office of Science, Basic Energy Sciences, Division of Materials Sciences and Engineering, under contract no. DE-FG02-09ER46056.